DOI: https://doi.org/10.15407/techned2023.03.022

SIMULATION AND EXPERIMENTAL INVESTIGATION OF DUAL THREE-PHASE BLDC MOTOR OPERATION AT IMBALANCED MODULAR LOADING

I.Z. Shchur[*], B.M. Kharchyshyn[**], V.P. Turkovskyi[***]
Lviv Polytechnic National University,
12, S. Bandera str., 79013, Lviv, Ukraine.
E-mail: ihor.z.shchur@lpnu.ua; bohdan.m.kharchyshyn@lpnu.ua; valentyn.p.turkovskyi@lpnu.ua

Electric machines built according to the modular principle – with several three-phase windings on a stator – are a new direction of modern electromechanics, because they have a number of advantages compared to traditional single-winding machines. Among these benefits, the most important are increased efficiency and fault tolerance, which is especially important for self-powered electric vehicles. However, the presence of a mutual magnetic coupling between the modules, as well as their unequal electrical load, amplify the electromagnetic torque ripple inherent in one or another electric drive system. In this work, the electromagnetic torque ripples in a dual three-phase (DTP) brushless DC motor (BLDCM) under different loads of its modules were investigated for the cases of absence and presence of mutual magnetic coupling between armature winding sets and in the cases of the drive operation in open and closed control systems. The research was carried out by means of simulation in the Matlab/Simulink environment on a circular model of real mock-up sample of DTP permanent magnet machine developed based on the results of its magnetic field simulation using the finite element method. Adequacy of simulation results is confirmed by experimental investigation. The results of the DTP BLDCM simulation studies showed an increase in the relative electromagnetic torque ripples of individual modules due to both the presence of magnetic coupling between winding sets and the deviation from their equal loading. However, at the level of the whole DTP BLDCM, a significant mutual compensation the electromagnetic torque ripples of the modules is shown, especially if they are magnetically coupled. The presence of closed-loop control systems of individual modules significantly reduces the electromagnetic torque ripples caused by different loading of the modules, especially in the case of magnetically uncoupled modules. References 26, figures 7, tables 3.
***Keywords**:* brushless DC motor (BLDCM), dual three-phase BLDCM, magnetic coupling, electromagnetic torque ripple, imbalanced modular loading, control system.

Introduction. The growing interest in development of electric drive and power supply systems by the modular principle has become a recent trend [1–3]. This interest is due to many advantages of modular approach that are particularly important for autonomous vehicles for land, air, and water applications, where increased reliability due to fault tolerance, redundancy, and safety is a priority [4–7]. In addition, the modular implementation of powertrain systems has many technical and economic advantages over their traditional configuration: reduced power of one phase of the electric machine, reduced supply voltage, increased energy efficiency, the possibility of multilevel and multifunctional control, lower interference, improved maintainability, and cheaper production [8, 9].

One of the first options for implementing a modular approach is multiphase electric machines, including multiple three-phase machines [10, 11]. Among them, dual three-phase (DTP) machines are the most common due to their simplicity and ability to apply all advantages of three-phase machines [7, 12], [13]. According to this configuration, first, only powerful asynchronous drives were implemented, then synchronous machines with permanent magnets (PM), and recently also brushless DC motors (BLDCM) [14–16]. Using a modular electric drive based on a DTP PM machine is associated with specific hardware and software complications of the entire system. However, this is less true for a DTP BLDCM due to the known advantages of this drive: a more straightforward design of an electric machine with PMs placed on the rotor surface, cheap point sensors of the rotor angular position, discrete low-frequency switching of

ORCID ID: [*] https://orcid.org/0000-0001-7346-1463; [**] https://orcid.org/0000-0001-6314-2637;
[***] https://orcid.org/0000-0001-9456-2394

armature windings, and simple control system [17]. Therefore, due to the advantages of the DTP concept, DTP BLDCMs are becoming promising for simple and cheap vehicles of lower power.

In DTP electric machines, especially with asymmetric configuration (with the optimal angular shift between the modules of the stator winding), due to the existing of magnetic coupling between these modules, additional current pulsations are generated, which leads to corresponding ripples of the electromagnetic torque [9–11, 18]. Such pulsations increase even more in the case of an unequal electrical load of two modules, which necessitates the use of special additional systems for equalizing their currents or electromagnetic torques [19, 20]. In the DTP BLDCM, the traditional pulsations of currents associated with the low-frequency position switching of armature winding sets are also added to these ripples. Reduction of BLDCM torque ripple caused by pulsations of armature currents due to their commutation devoted many works [21, 22]. In the same time, the task of investigation of magnetically interconnected processes of time-spaced positional switching of the DTP BLDCM armature winding modules under different electromagnetic loads of these modules, as far as the authors know, has not yet been solved.

The purpose of this work is to estimate the electromagnetic torque ripples in the DTP BLDCM at different imbalanced loads of the armature winding modules. The study was conducted by computer simulation in Matlab/Simulink. To do this, a computer model of the DTP PM machine was used, which was created based on a circular mathematical model of this machine developed by modeling the magnetic field of an actual sample of the machine by finite element method (FEM) [18, 23]. Some of the results were confirmed by experimental studies on a DTP BLDCM mock-up sample.

1. Configuration of DTP BLDCM drive and design of PM DTP machine. The asymmetric DTP PM machine M (Fig. 1) has two modules of the armature winding sets 1-2-3 and 4-5-6 spatially shifted by $\gamma = 30^{o}$ el. with isolated neutral points that eliminates the pulsating of the sixth harmonic in the electromagnetic torque [9].

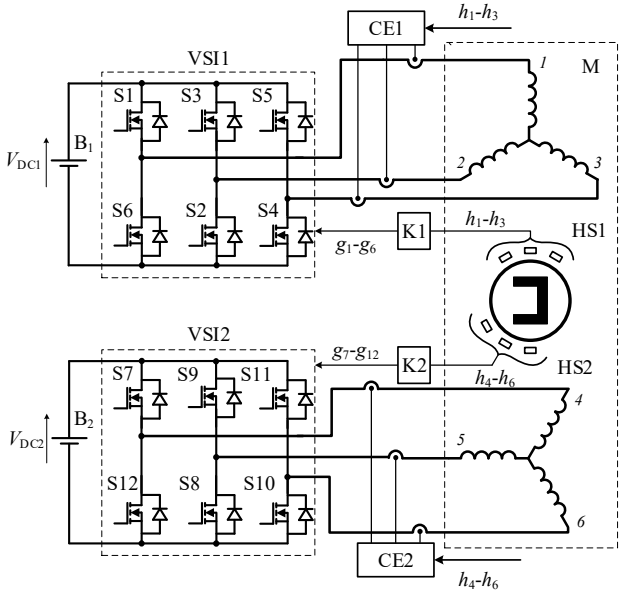

Fig. 1

In the DTP BLDCM, voltage source inverters VSI1 and VSI2 provide the switching of each three-phase armature-winding set of the DTP PM machine M. This switching is synchronized with the current position of the rotor by the signals g_1-g_6 and g_7-g_{12} received, respectively, from their sets of discrete Hall sensors HS1 and HS2 with output signals h_1-h_3 and h_4-h_6 of the rotor angular position (Fig. 1). Each DTP armature winding set of the PM machine is switched according to the traditional for a BLDCM 120-degree principle of switch conductivity [17]. The commutation algorithm of the invertors VSI1 and VSI2 switches depending on the rotor position angle θ in el. degree for the DTP PM machine of asymmetrical configuration with the displacement of the armature winding sets by 30^{o} el. is presented in Table 1 [18]. Voltage inverters are powered by their DC sources such as batteries B1 and B2 with voltages V_{DC1} and V_{DC2} respectively.

The implementation of the DTP PM machine armature can be magnetically insulated for each module or common to both modules of the machine. Since in the latter case much higher specific values of torque and power are achieved, it is most often used. Concentrated windings with non-intersecting frontal parts are also used, and the reduction of mutual inductive coupling between the armature winding sets and the reduction of electromagnetic torque ripples are provided by using fractional-slot concentrated windings [24]. These windings have the advantages over traditional distributed windings as high winding ratio and short front parts of the winding. That provides better use of copper and reduces energy loss, reduced probability of interphase short circuit, and low toothed torque [25]. However, windings with fractional slots generate a large number of spatial harmonics of the stator magnetomotive force.

Table 1

θ (° el.)	Switching states												θ (° el.)
	VSI1						VSI2						
	S1	S2	S3	S4	S5	S6	S7	S8	S9	S10	S11	S12	
0 - 30	1	1	0	0	0	0	1	1	0	0	0	0	0 - 30
30 - 60							1	0	0	1	0	0	30 - 60
60 - 90	1	0	0	1	0	0							60 - 90
90 - 120							0	0	1	1	0	0	90 - 120
120 - 150	0	0	1	1	0	0							120 - 150
150 - 180							0	0	1	0	0	1	150 - 180
180 - 210	0	0	1	0	0	1							180 - 210
210 - 240							0	0	0	0	1	1	210 - 240
240 - 270	0	0	0	0	1	1							240 - 270
270 - 300							0	1	0	0	1	0	270 - 300
300 - 330	0	1	0	0	1	0							300 - 330
330 - 360							1	1	0	0	0	0	330 - 360

2. Circular mathematical model of the DTP PM machine. In further investigation, based on previous studies [26], we used a circular mathematical model of an asymmetric DTP RM machine developed in [18]. The parameters of this machine of the fractional slot structure $Z / 2p / i = 24/20/3$ are given in Table 2. They correspond to the real mock-up sample of this machine and are determined either experimentally or by the results of FEM modeling the magnetic field of this machine [23]. In order to simplify the circular mathematical model, several assumptions given in [18] are accepted; in particular, the dependences of the self and mutual inductances on the rotor position angle and the saturation of the magnetic field were neglected.

Table 2

Parameters	Value
Rated power P_n (W)	300
Supply DC voltage V_{DC} (V)	48
Rated angular velocity, ω_n (s^{-1})	20
Rated torque T_n (Nm)	15
Number pair of poles p	10
Moment of inertia J ($kg \cdot m^2$)	0.1
Per module:	
Winding resistance R (Ω)	0.25
Winding self inductance L (mH)	5.39
Winding mutual inductance, M (mH)	1.59
Flux linkage by PM ψ_{pm} (Wb)	0.112

Under made assumptions, the voltage equilibrium in all phase circuits of the DTP armature winding is described by the following vector-matrix equation [18]:

$$\vec{v} = \mathbf{R}\,\vec{i} + \mathbf{L}\frac{d}{dt}\vec{i} + \vec{e}, \qquad (1)$$

where $\vec{v}$, $\vec{i}$, $\vec{e}$ are the vectors-columns of the phase voltages, currents and EMFs, respectively, consisting of six elements; **R** is the diagonal matrix of identical resistances R of the phase winding; **L** is the matrix of static inductances.

The matrix **L** can be represented as the sum of two matrices: $\mathbf{L_a}$, which reflects the operation of each of the winding set connected in a star taking into account its own interphase mutual inductance, but without taking into account the mutual inductive connections between the phases of the two winding sets, and **M**, which describes exactly the mutual inductances between the winding sets [23]:

$$\mathbf{L} = \mathbf{L_a} + \mathbf{M} = \mathrm{diag}_6\left[L_a\right] + M\begin{bmatrix} 0 & 0 & 0 & \cos\gamma & 0 & -\cos\gamma \\ 0 & 0 & 0 & -\cos\gamma & \cos\gamma & 0 \\ 0 & 0 & 0 & 0 & -\cos\gamma & \cos\gamma \\ \cos\gamma & -\cos\gamma & 0 & 0 & 0 & 0 \\ 0 & \cos\gamma & -\cos\gamma & 0 & 0 & 0 \\ -\cos\gamma & 0 & \cos\gamma & 0 & 0 & 0 \end{bmatrix}, \qquad (2)$$

where L and M are the self and mutual inductances of one set of armature winding, respectively; $L_a = L - M$.

The electromagnetic torque of the DTP PM machine can be presented as

$$T_e = \left(\vec{e} \cdot \vec{i}\right)\omega^{-1}, \qquad (3)$$

where $\left(\vec{e} \cdot \vec{i}\right)$ is the dot product of the vectors of EMF and armature current and ω is the motor angular velocity.

The equation of motion of a drive for the single-mass mechanical system with the related to the motor shaft moment of inertia J_Σ has the form:

$$J_\Sigma \frac{d\omega}{dt} = T_e - T_L - b\omega \ , \tag{4}$$

where T_L is the load torque of the drive; b is the coefficient of viscous friction.

The position angle of the machine rotor is determined by equation:

$$\theta = \int \omega \, dt \, . \tag{5}$$

The parameters of the voltage vector applied to the armature windings in (1) depend on the method of DTP PM machine control. Due to the complexity of the mathematical description of the switching processes of each winding set of the DTP PM machine, mathematical modeling of the modular BLDC drive operation should be performed by computer simulation in the Matlab/Simulink software using virtual models of VSIs and six-step switching algorithms, which is presented in Table 1.

3. MATLAB/Simulink model of the DTP BLDCM drive. The developed in Matlab/Simulink model of the DTP BLDCM drive shown in Fig. 2 is similar to the one created in [18]. It consists of two similar parts, in which the subsystems and main blocks are marked by indices 1 and 2. In each part, the electromagnetic part of the PM machine module is represented by the PM Machine Module Subsystem, which is switched by its six-switch VSI powered by its Battery Subsystem according to Figure 1. The PWM Subsystem generates the control signals for the VSI switches according to Table 1 based on "pulses" signals produced by the Hall Subsystem. Because of asymmetrical configuration of two armature-winding modules, the switching of the VSI2 is shifted by an angle of $\pi/6$ relative to the VSI1. The PWM Subsystem adjusts the output VSI voltage in proportion to the input reference signal by PWM of three lower switches of the inverter. The DTP BLDCM drive operates in a closed two-loop control system with an outer loop of the angular velocity control by proportional speed regulator SR (k_P = 20) and inner two loops of the current control for each machine module by PI current regulators CR (k_P = 10, k_I = 500). For making the current feedbacks, in each part, the estimated equivalent DC current value of winding set was obtained by the Current Estimator based on the phase currents of winding set and the signals from the rotor position sensors g_1-g_3 or g_4-g_6 (see Fig. 1) [3]. Finally, the electromagnetic torques generated by two machine modules are added. Obtained total electromagnetic torque goes to the common mechanical part of the drive, which is implemented in accordance with (4) and (5). The models of all subsystems of the developed model of the DTP BLDCM drive are the same as in [18].

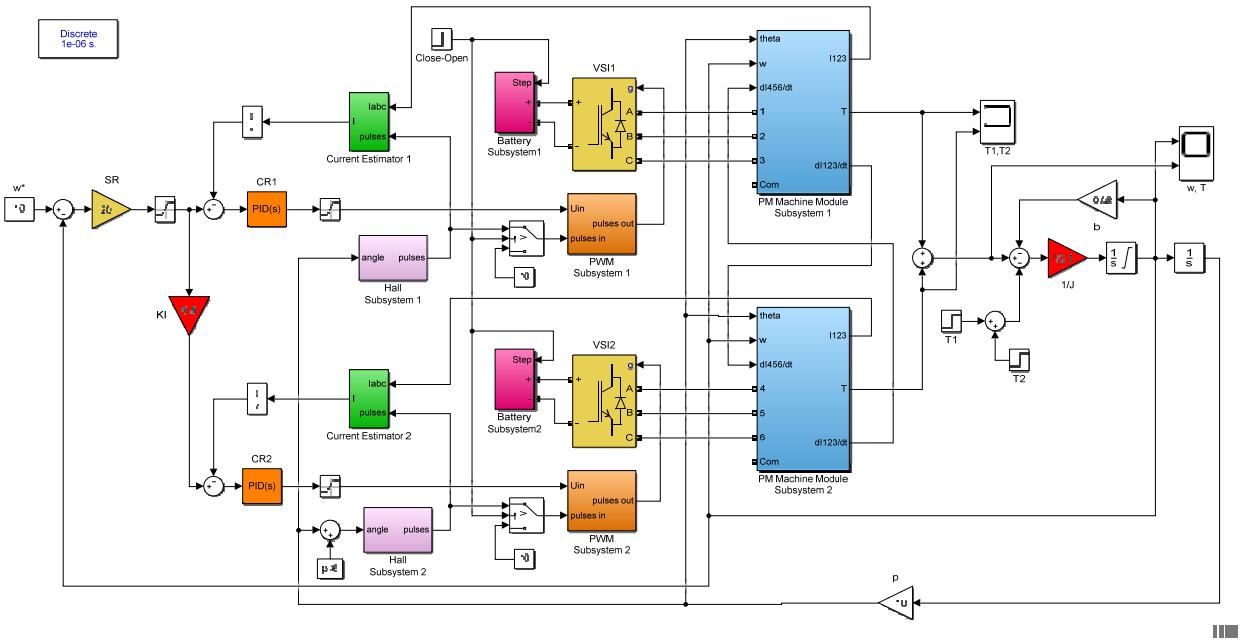

Fig. 2

The developed computer model DTP BLDCM drive allows electromagnetic loading of two PM machine modules in different ratios. It is chosen that the second machine module always have a less load, i.e. it will create less electromagnetic torque than the first module.

For research of the DTP BLDCM drive operation in the open system, after fast acceleration of the motor to the reference angular velocity in the closed-loop system, the Close-Open block provides the following switching in the system. The inputs of the two PWM Subsystems are switched over the maximum PWM value of 10, at which the speed and current feedbacks stop operation. In addition, based on the signal from the same block Close-Open, the corresponding switches in both Battery Subsystems switch the batteries voltages from the nominal value $V_{B1.n} = V_{B2.n} = 48$ V to new values that correspond to the specified set ratio $K_V = V_{B2} / V_{B1}$. In this case, the absolute values of voltages V_{B1} and V_{B2} are pre-selected on the model to ensure the same value of the specified angular velocity of the motor as in the closed system.

For investigation of the DTP BLDCM drive operation with various loadings of modules in the closed-loop control system, it is enough to set the necessary ratio of currents in two winding sets $K_I = I_2 / I_1$ in the KI block, which connects the output of the speed regulator with the reference current (electromagnetic torque) of the second module.

4. Simulation results and discussion. In the simulation process, the influence of different electromagnetic loads of the machine modules on the electromagnetic torque ripples generated by them, as well as the on the total electromagnetic torque of the DTP BLDCM during the drive operation in open and closed-loop control systems was evaluated. The studies were performed at a constant average value of the motor angular velocity of 10 rad/s. To compare the level of the electromagnetic torque ripple, the absolute torque ripple ΔT_e and its relation to the average torque value $T_{e\,ave}$ in the steady-state operation of the drive were estimated:

$$\delta T_e = \frac{\Delta T_e}{T_{e\,ave}} = \frac{T_{e\max} - T_{e\min}}{T_{e\,ave}} \qquad (6)$$

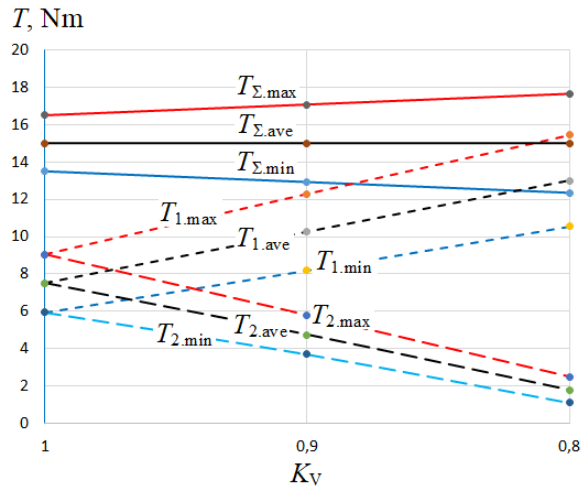

Fig. 3

Fig. 3 shows one of the results of the study, in particular, the dependences of the minimum, average, and maximum values of electromagnetic torques of the first T_1 and second T_2 modules, as well as the total electromagnetic torque T_Σ of the DTP BLDCM on the ratio of DC supply voltages of module inverters K_V in the open system for the case of magnetically insulated winding sets. As can be seen from the obtained dependences, already at a value of approximately $K_V = 0.75$, the electromagnetic torque generated by the second module is reduced to zero, and the entire electromagnetic torque of the drive is formed by the first module only. This is because the phase voltages of the second armature winding become less than the phase EMFs of rotation of this winding. As the K_V increases, the electromagnetic torque ripples of the first module and the whole drive also increase. Because of this, further estimation of electromagnetic torque ripples was performed for a value of $K_V = 0.8$ in the open system and $K_I = 0.8$ in the closed-loop control system. The research results are summarized in Table 3, where in the numerator of each cell is the result for the open system, and in the denominator of each cell is the result for the closed-loop system.

Analysis of the simulation results shows the following.

With the same load of two modules in the case of an open system drive, the relative electromagnetic torque ripples generated by each module are almost as twice large in the case of magnetically coupled winding sets as in the absence of magnetic coupling between the modules. However, the total electromagnetic torque ripples in both cases remain almost equal. A similar pattern is also observed in the case when the electromagnetic load of the two modules differs by 20%. However, in this case, the total electromagnetic torque ripples for magnetically coupled winding sets are significantly reduced (from 35.3 to 25.3%) compared to the lack of mutual inductance between the modules.

Table 3

Presence of magnetic coupling between modules	Load of the armature winding modules	Module 1			Module 2			DTP BLDCM	
		$T_{e\,ave}$ (N·m)	ΔT_e (N·m)	δT_e (%)	$T_{e\,ave}$ (N·m)	ΔT_e (N·m)	δT_e (%)	ΔT_e (N·m)	δT_e (%)
Magnetically uncoupled	Equal load of modules	7.5 / 7.5	3.1 / 2.5	41.3 / 33.3	7.5 / 7.5	3.1 / 2.5	41.3 / 33.3	2.0 / 3.2	13.3 / 21.3
	Different load of modules	13.0 / 8.3	4.9 / 2.5	37.7 / 30.1	2.0 / 6.7	1.4 / 2.0	70.0 / 29.9	5.3 / 2.2	35.3 / 14.7
Magnetically coupled	Equal load of modules	7.5 / 7.5	5.6 / 2.5	74.7 / 33.3	7.5 / 7.5	5.6 / 2.5	74.7 / 33.3	2.0 / 3.0	13.3 / 20.0
	Different load of modules	13.0 / 8.4	6.0 / 2.8	46.1 / 33.3	2.0 / 6.6	3.0 / 2.4	150 / 36.4	3.8 / 3.0	25.3 / 20.0

In the case of the DTP BLDCM operation in the closed-loop control system, with the same load of the modules, the electromagnetic torque ripples do not depend on the presence or absence of magnetic interconnection between the modules. When the electromagnetic load of the two modules differs by 20%, the relative ripples of the electromagnetic torque increase (from 14.7% to 20.0%) in the case of magnetically coupled winding sets compared to the lack of mutual inductance between the modules.

Fig. 4 shows the time diagrams of the main variables of the DTP BLDCM drive, obtained in simulation for the cases of without (left) and with (right) presence of magnetic interconnection between the armature winding sets. In both cases, the drive worked on the same program. Initially, the DTP BLDCM worked in the closed-loop control system, but with a different electromagnetic load of the modules, which was provided by a value of $K_I = 0.8$. Approximately, up to 0.04 s, the motor accelerated with a static torque load equal to 1/3 of the rated value, and at a time of 0.07 s additionally applied the static torque load to the rated value. In 0.12 s, the electric drive system opened, and then the DTP BLDCM worked at the previous speed, but with a different load, which was provided by the value of $K_V = 0.8$ (Fig. 4, *a*).

The time diagrams obtained show that the simulated difference in electromagnetic load of two modules of the DTP BLDCM, which was estimated at $K_I = 0.8$ in the closed system and $K_V = 0.8$ in the open system, is very different – in the second case, this difference is much larger. Comparison of the same time diagrams for cases with and without mutual induction between the winding sets makes it possible to follow all indicators of the electromagnetic torque ripples, which are given in Table 3. In particular, from Fig. 4, *b*, it would be seen that the total electromagnetic torque has smaller ripples at the absence of mutual induction between winding sets in the closed-loop system and at the presence of mutual induction in the open system, although the electromagnetic torque ripples of modules in the latter case are larger (Fig. 4, *c*). This dependence can be seen from the time diagrams of the currents in the close phases of both winding sets, 1 – more loaded and 4 – less loaded, together with their phase EMFs for both studied cases, which are shown in Figs. 4, *d* and 4, *e*, respectively. They also show that the switching of the two winding sets is clearly based on the principle of 120-degree of conductivity of the inverter switches and in accordance with the phase EMFs. The EMFs have a shape, which is slightly different from the sinusoidal one, with the presence of the third harmonic at a level of 9.3% from the first harmonic, which corresponds to the real EMF form of the investigated sample of DTP PM machine.

Time diagrams of currents in in Fig. 4, *d* and 4, *e*, respectively.

5. Experimental investigation of the DTP BLDCM drive operation. For the experimental study, the developed mock-up sample of DTP BLDCM drive with the DTP PM machine *1* of asymmetric module configuration and external rotor was used (Fig. 5). Parameters of this DTP BLDCM drive are shown in Table 2. A brush DC motor *2* created the static torque load on a shaft of the investigated machine.

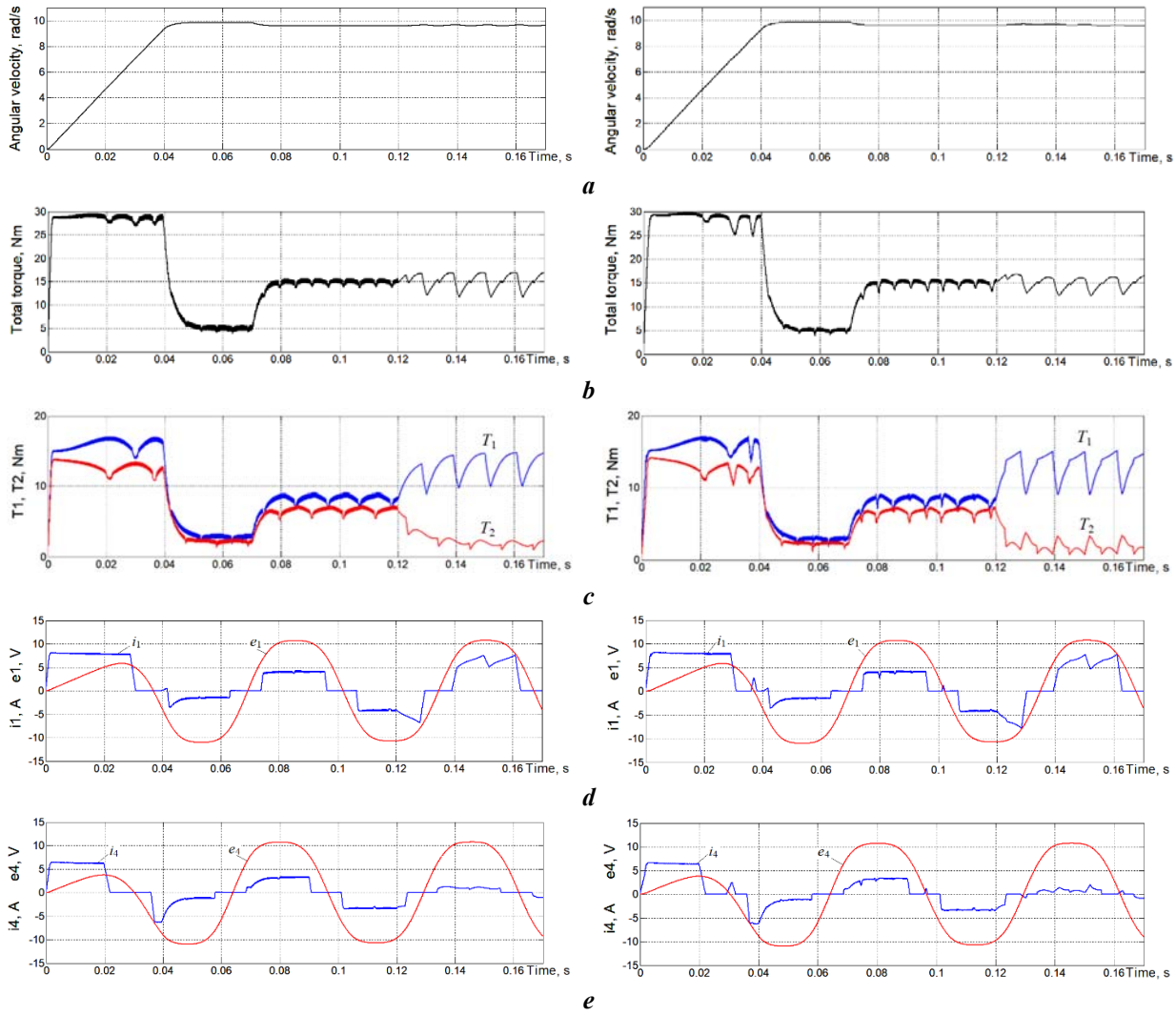

Fig. 4

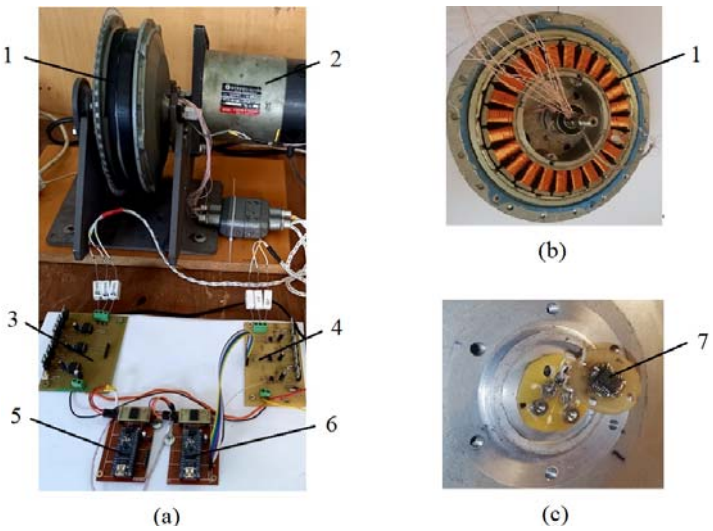

Fig. 5

As a rotor position sensor, a miniature absolute magnetic semiconductor encoder AS5045 with a 12-bit code is used (*7* in Fig. 5, *c*), from which the discrete signals synchronized with the EMFs of two armature winding sets with the displacement by 30° el. were obtained. Two VSIs *3* and *4* are built on MOSFET IRF3205 with IR2104 drivers. Switching of each of the armature winding modules was carried out using its microcontroller Arduino PRO mini Atmega168 *5* and *6* based on the signals of the angular position of the rotor. Separate power supplies (not shown in Fig. 5) provided DC supply voltage of the DTP BLDCM modules.

Figs. 6 and 7 show the experimentally obtained waveforms of the voltage and current in the phases of the same name (*1* and *4* in Fig. 1) of the studied DTP BLDCM, which operated in the open system at the equal (Fig. 6, *a*) and different (Fig. 7) loads of two machine modules. For comparison, Fig. 6, *b* shows similar time diagrams of the voltage and current in phase 1 obtained in simulation. The same trends of changes and forms of phase voltages and

currents in the experimental and model results shown in Fig. 6, and the difference between them up to 15% confirm the adequacy of the developed computer model of the studied DTP BLDCM with inductive coupling between two armature winding sets.

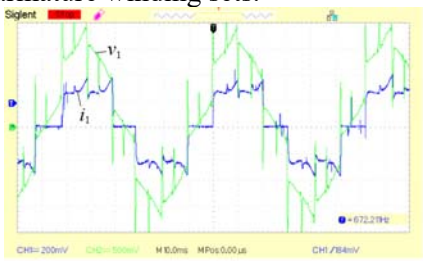

a

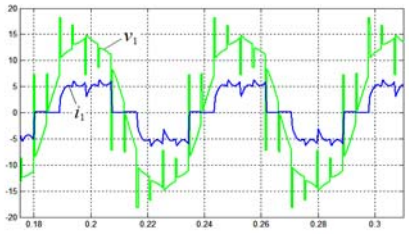

b

Fig. 6

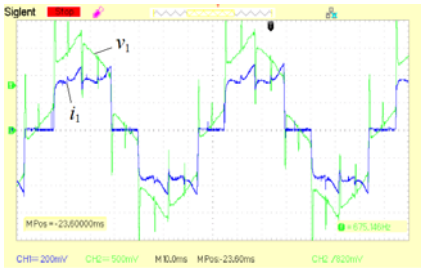

a

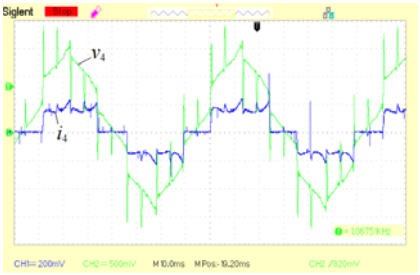

b

Fig. 7

Conclusions.

Modular electric machines, in particular, those consisting of separate three-phase winding sets, attract the interest of researchers due to the improvement of the efficiency of modular electric drives and ensuring their fault tolerance. In BLDCMs, the asymmetrical modular configuration of the armature winding also ensures the reduction of switching ripples of the total electromagnetic torque if the three-phase modules are optimally spaced. On the other hand, as is known, the uneven electromagnetic loading of the modules leads to an increase of the machine's electromagnetic torque ripples. In this work, the effect of uneven loading of the DTP BLDCM modules with different magnetic coupling on the pulsations of electromagnetic torques created both by individual machine modules and the total of the entire machine is studied in detail.

Both investigated factors – the presence of mutual inductance between the armature windings of two machine modules and difference in the electromagnetic loading of these modules – lead to an increase in the pulsations of the electromagnetic torques of individual machine modules. However, at the level of the total electromagnetic torque of the entire DTP BLDCM, the result changes. For the same load of the machine modules, regardless of the increase in the pulsations of the electromagnetic torques of individual modules, the relative total electromagnetic torque ripple of the machine remain the same and equal to 13.3% for the cases of magnetically isolated and magnetically coupled machine modules. With the different load of the modules (20% difference), the total electromagnetic torque ripple is reduced by 28.3% for the case of magnetically coupled modules in comparison with magnetically isolated machine modules. This indicates that the mutual inductive coupling between the armature winding sets in DTP BLDCM causes such additional pulsations of the electromagnetic torques of the modules, which are characterized by good mutual compensation, which is a valid conclusion from the conducted research.

In the case of the DTP BLDCM operation in the closed control system, the electromagnetic torque ripples both in individual modules and in the whole drive practically do not depend on the degree of deviation from the equality of machine modules loading and remain relatively low due to the current control systems in the armature winding sets.

The results of experimental studies conducted on the created DTP BLDCM mock-up sample showed their good agreement with those obtained during the computer simulation with a maximum difference of up to 15%. This confirms the adequacy of the developed mathematical models of the DTP BLDCM of asymmetric configuration with magnetic coupling between armature winding sets.

Роботу виконано за кошти бюджетної програми "Розвиток модульного інтегрованого підходу до конфігурування та керування бортових систем електроприводу та електричного живлення автономних транспортних засобів" (ЕАТЗ, 0120U102206), КПКВК 2201040.

1. Stippich A., van der Broeck C.H., Sewergin A., Wienhausen A.H., Neubert M., Schulting P., Taraborrelli S., van Hoek H., De Doncker R.W. Key components of modular propulsion systems for next generation electric vehicles. *CPSS Transactions on Power Electronics and Applications*. 2017. Vol. 2. Is. 4. Pp. 249–258. DOI: https://doi.org/10.24295/CPSSTPEA.2017.00023
2. Galassini A., Costabeber A., Gerada C., Buticchi G., Barater D. A modular speed-drooped system for high reliability integrated modular motor drives. *IEEE Transactions on Industry Application*. 2016. Vol. 52. Is. 4. Pp. 3124–3132. DOI: https://doi.org/10.1109/TIA.2016.2540608
3. Shchur I., Turkovskyi V. Integrated system of modular power supply and multilevel control of brushless DC motor for electric vehicles. *Naukovyi Visnyk Natsionalnoho Hirnychoho Universytetu*. 2020. Vol. 6. Pp. 107–115. DOI: https://doi.org/10.33271/nvngu/2020-6/068
4. Salem A., Narimani M.A. Review on multiphase drives for automotive traction applications. *IEEE Transactions on Transportation Electrification*. 2019. Vol. 5. Is. 4. Pp. 1329–1348. DOI: https://doi.org/10.1109/TTE.2019.2956355
5. Kuznetsov B., Bovdui I., Nikitina T., Kolomiets V., Kobilyanskiy B. Multi-motor plant related electric drives robust control synthesis. Proceedings of the 2020 IEEE 4th International Conference on *Intelligent Energy and Power Systems (*IEPS). Istanbul, Turkey, September 07-11, 2020. Pp. 242–245. DOI: https://doi.org/10.1109/IEPS51250.2020.9263169
6. Zhao W., Xu L., Liu G. Overview of permanent-magnet fault-tolerant machines: Topology and design. *CES Transactions on Electrical Machines and Systems*. 2018. Vol. 2. Is. 1. Pp. 51–64. DOI: https://doi.org/10.23919/TEMS.2018.8326451
7. Hasoun M., El Afia A., Khafallah M., Benkirane K. Experimental implementation a PWM strategy for dual three-phase PMSM using 12-sector vector space decomposition applied on electric ship propulsion. *International Journal of Power Electronics and Drive Systems (IJPEDS)*. 2020. Vol. 11. No 4. Pp. 1701–1710. DOI: https://doi.org/10.11591/ijpeds.v11.i4.pp1701-1710
8. Shchur I., Kasha L., Bukavyn M. Efficiency evaluation of single and modular cascade machines operation in electric vehicle. Proceedings of the IEEE 15th International Conference on *Advanced Trends in Radioelectronics, Telecommunications and Computer Engineering* (TCSET). Lviv–Slavske, Ukraine, February 25-29, 2020. Pp. 156–161. DOI: https://doi.org/10.1109/tcset49122.2020.235413
9. Patel V.I., Wang J., Nugraha D.T., Vuletić R., Tousen J. Enhanced availability of drivetrain through novel multiphase permanent-magnet machine drive. *IEEE Transactions on Industrial Electronics*. 2015. Vol. 63. No 1. Pp. 469–480. DOI: https://doi.org/10.1109/TIE.2015.2435371
10. Muqorobin A., Dahono P. A. Study of current ripple characteristics of inverter-fed multiple three-phase alternating current motors. *International Journal of Power Electronics and Drive Systems (IJPEDS)*. 2022. Vol. 13. No 1. Pp. 68–83. DOI: https://doi.org/10.11591/ijpeds.v13.i1.pp68-83
11. Zoric I., Jones M., Levi E. Arbitrary power sharing among three-phase winding sets of multiphase machines. *IEEE Transactions on Industrial Electronics*. 2018. Vol. 65. No 2. Pp. 1128–1139. DOI: https://doi.org/10.1109/TIE.2017.2733468
12. Hu M., Hua W., Zhang H., Zhao G., Ma G., Xu S. Modeling and control of a dual three-phase permanent magnet machine accounting for asymmetry between two winding sets. Proceedings of the International Conference on *Electrical Machines* (ICEM). Gothenburg, Sweden, August 23-26, 2020. Pp. 2111–2117. DOI: https://doi.org/10.1109/ICEM49940.2020.9270708
13. Eldeeb H., Abdelrahem M., Hackl C., Abdel-Khalik A.S. Enhanced electromechanical modeling of asymmetrical dual three-phase IPMSM drives. Proceedings of the 27th IEEE International Symposium on *Industrial Electronics* (ISIE). Cairns, Australia, June 12-15, 2018. Pp. 126–132. DOI: https://doi.org/10.1109/ISIE.2018.8433755
14. Fu Z., Liu J., Xing Z. Performance analysis of dual-redundancy brushless DC motor. *Energy Reports*. 2020. No 6. Pp. 829–833. DOI: https://doi.org/10.1016/j.egyr.2020.11.125
15. Bogusz P., Korkosz M., Prokop J. A study of dual-channel brushless DC motor with permanent magnets. Proceedings of the *2016 13th Selected Issues of Electrical Engineering and Electronics* WZEE. Rzeszow, Poland, May 4-8, 2016. Pp.1-6. DOI: https://doi.org/10.1109/WZEE.2016.7800189
16. Shchur I., Turkovskyi V. Open-end winding dual three-phase BLDC motor drive system with integrated hybrid battery-supercapacitor energy storage. Proceedings of the IEEE International Conference on *Modern Electrical and Energy Systems* (MEES). Kremenchuk, Ukraine, September 21-24, 2021. Pp. 1-6. DOI: https://doi.org/10.1109/MEES52427.2021.9598697
17. Mozaffari Niapour S.A.KH., Shokri Garjan GH., Shafiei M., Feyzi M.R., Danyali S., Bahrami Kouhshahi M. Review of permanent-magnet brushless DC motor basic drives based on analysis and simulation study. *International Review of Electrical Engineering* (IREE). 2014. Vol. 9 (5). Pp. 930–957. DOI: https://doi.org/10.15866/iree.v9i5.827
18. Shchur I., Jancarczyk D. Electromagnetic torque ripple in multiple three-phase brushless DC motors for electric vehicles. *Electronics*. 2021. Vol. 10 (24). 3097. Pp. 1–25. DOI: https://doi.org/10.3390/electronics10243097

19. Yan H., Xu Y., Zou J., Wang B., Jiang S. A maximum current sharing method for dual-redundancy brushless DC Motor control. Proceedings of the 17th International Conference on *Electrical Machines and Systems* (ICEMS). Hangzhou, China, October 22-25, 2014. Pp. 1057–1061. DOI: https://doi.org/10.1109/ICEMS.2014.7013634
20. Bian C., Li X., Zhao G. The peak current control of permanent magnet brushless DC machine with asymmetric dual-three phases. *CES Transactions on Electrical Machines and Systems*. 2018. Vol. 2. Pp. 29–135. DOI: https://doi.org/10.23919/TEMS.2018.8326459
21. Mahalingam K., Chellaiah Ramji N.K. A comparative analysis of torque ripple reduction techniques for sensor BLDC drive. *International Journal of Power Electronics and Drive Systems* (IJPEDS). 2022. Vol. 13. No 1. Pp. 122–131. DOI: https://doi.org/10.11591/ijpeds.v13.i1.pp122-131
22. Krishnakumar V., Madhanakkumar N., Pugazhendiran P., Bharathiraja C., Sriramkumar V. Torque ripple minimization of PMBLDC motor using simple boost inverter. *International Journal of Power Electronics and Drive Systems* (IJPEDS). 2019. Vol. 10. No 4. Pp. 1714–1723. DOI: https://doi.org/10.11591/ijpeds.v10.i4.pp1714-1723
23. Makarchuk O., Kharchyshyn B., Kasha L. Analysis of the magneto-mechanical characteristic of double three-phase PMSM. Proceedings of the IEEE 3rd Ukraine Conference on *Electrical and Computer Engineering* (UKRCON). Lviv, Ukraine, August 26-28, 2021. Pp. 333–338. DOI: https://doi.org/10.1109/UKRCON53503.2021.9575684
24. Li G. J., Ren B., Zhu Z. Q. Design guidelines for fractional slot multi-phase modular permanent magnet machines. *IET Electric Power Applications*. 2017. Vol. 11. Pp. 1023–1031. DOI: https://doi.org/10.1049/iet-epa.2016.0616
25. Yokoi Y., Higuchi T., Miyamoto Y. General formulation of winding factor for fractional-slot concentrated winding design. *IET Electric Power Applications*. 2016. Vol. 10. Pp. 231–239. DOI: https://doi.org/10.1049/iet-epa.2015.0092
26. Shchur I., Rusek A., Makarchuk O., Lis M. The simulation model of a synchronous machine with permanent magnets that takes into account magnetic saturation. *Przegląd Elektrotechniczny (Electrical Review)*. 2013. No 4. Pp. 102–105. URL: http://pe.org.pl/articles/2013/4/22.pdf (accessed at 25.09.2022).

УДК 621.313.5.8

МОДЕЛЮВАННЯ ТА ЕКСПЕРИМЕНТАЛЬНЕ ДОСЛІДЖЕННЯ ДВОМОДУЛЬНОГО ТРИФАЗНОГО БЕЗЩІТКОВОГО ДВИГУНА ПОСТІЙНОГО СТРУМУ ЗА НЕЗБАЛАНСОВАНОГО МОДУЛЬНОГО НАВАНТАЖЕННЯ

І.З. Щур, докт. техн. наук, **Б.М. Харчишин,** канд. техн. наук, **В.П. Турковський**
[1]Національний університет „Львівська політехніка”,
вул. С. Бандери 12, Львів, 79013, Україна.
E-mail: ihor.z.shchur@lpnu.ua, bohdan.m.kharchyshyn@lpnu.ua, valentyn.p.turkovskyi@lpnu.ua

Електричні машини, побудовані за модульним принципом – з кількома трифазними обмотками на статорі, є новим напрямком сучасної електромеханіки, оскільки мають низку переваг у порівнянні з традиційними однообмотковими машинами. Серед цих переваг найважливішими є підвищення енергетичної ефективності та стійкості до відмов, що є особливо важливим для електричних транспортних засобів з автономним живленням. Проте наявність взаємоіндуктивного зв’язку між модулями, а також їхнє неоднакове електричне навантаження підсилюють пульсації електромагнітного моменту, притаманні тій чи іншій системі електропривода. У роботі досліджено пульсації електромагнітного моменту в двомодульному безщітковому двигуні постійного струму (БДПС) за різних навантажень його модулів у випадках відсутності та наявності взаємного магнітного зв’язку між комплектами обмотки якоря, а також у випадках роботи привода у розімкненій та замкненій системах керування. Дослідження проводили шляхом моделювання в середовищі Matlab/Simulink на коловій моделі реального макетного зразку двомодульної машини з постійними магнітами, розробленій за результатами моделювання її магнітного поля методом скінченних елементів. Адекватність результатів моделювання підтверджено експериментальним дослідженням. Результати досліджень шляхом моделювання двомодульного БДПС показали збільшення відносних пульсацій електромагнітних моментів, створюваних окремими модулями як через наявність магнітного зв’язку між комплектами обмотки якоря, так і через відхилення від рівномірного навантаження модулів. Однак на рівні всього двомодульного БДПС показана значна взаємна компенсація пульсацій електромагнітних моментів модулів, особливо якщо вони магнітно зв’язані. Наявність замкнутих систем керування окремими модулями значно зменшує пульсації сумарного електромагнітного моменту, спричинені різним навантаженням модулів, особливо у випадку магнітно незв’язаних модулів. Бібл. 26, рис. 7, табл. 3.

Ключові слова: безщітковий двигун постійного струму (БДПС), двомодульний трифазний БДПС, магнітний зв’язок, пульсації електромагнітного моменту, незбалансоване модульне навантаження, система керування.

Надійшла 18.10.2022
Остаточний варіант 13.02.2023